

Synthesis and Characterization of Nano-Copper-Powder Based Magnetorheological Fluids for Brake

Chiranjit Sarkar¹, Harish Hirani²

¹Mechanical Engineering Department, Delhi Technological University, Delhi – 110042

²Mechanical Engineering Department, Indian Institute of Technology Delhi, New Delhi - 110016

Corresponding Email: chiranjit.ju@gmail.com

Abstract: *Magnetorheological (MR) fluids can be used as brake friction materials [1, 2]. During braking, kinetic energy of machines gets converted into heat and shear thinning of MR fluid due to increase in temperature occurs which in turn reduces the braking effect. To lessen the effect of heat generation on MR fluids due to heat, synthesis of magnetorheological fluid using nano-copper-powder has been proposed. To explore the feasibility of incorporating copper powder, four carbonyl iron (CI) powder based MR fluids (without any copper powder, with 0.25% weight, 0.5% weight and 0.75% weight copper powder) have been synthesized. Yield stress of all four MR fluids have been estimated using magnetorheometer.*

A flywheel based MR brake experimental setup has been developed to analyze the performance of synthesized MR fluids. To increase the braking torque of MR brake, compression mode along with the shear mode has been introduced. The comparison of the braking torque in shear and compression modes has been presented. “T” type thermocouples have been used to measure the temperature distribution of the fabricated MR brake. Results of braking torque and corresponding temperature distribution are presented.

Keywords — Magnetorheological fluids; Nano – copper powder; Shear mode; Compression mode; Temperature distribution

I. Introduction

MR fluid is a dispersion of micron sized pure iron particles in a non-magnetic fluid carrier [3, 4]. Under the presence of the magnetic field, particles form chains in the direction of magnetic flux and increase its yield stress. In MR brake [1-4], increase in fluid's yield stress restricts the rotational movement of disk and reduces the kinetic energy of the disk. The change in kinetic energy gets converted into heat that increases the temperature of MR fluid and shear thinning of MR fluid results. Shear thinning due to increase in temperature limits the usage of MR fluids in disk brakes [4-5].

The effects of temperature on the performance of MR devices have been explored by a number of researchers [5-7]. In experimental study on MR brake by Wang et al. [5], torque reduction from 300 Nm to 180 Nm on increasing operating temperature from 30°C to 180°C was observed. Weiss et al. [6] experimentally found that on increasing temperature from - 40 to 150°C, the plastic viscosity and dynamic yield stress of the

MR fluid decreased by 95 and 10%, respectively. Liao [7] witnessed sharp decay in the damping force of the MR damper when the temperature of the MR fluid increased from 20 to 80°C. To deal with shear thinning problem of MR devices due to heat, Wang et al. [5] proposed water cooling method. Dogruoz et al. [8] employed radiating fins in the shell to accelerate the heat dissipation from the MR fluid damper and control the temperature rise. Tian and Hou [9] proposed forced cooling of MR clutch. Zheng et al. [10] utilized rotary heat pipes to achieve forced cooling of the MR transmission device. Mistik et al. [11] synthesized and characterized MR fluids filled with spacer fabric. Their investigation showed that the thermal conductivity of the MR fluids with spacer fabric structures increased upon the application of magnetic field. In the present study, MR fluids with nano copper-powder have been synthesized to increase the heat transmission rate from the MR brake.

Four MR fluid samples have been synthesized using mechanical stirrer and then characterized using MCR-102 magnetorheometer at different temperatures. To confirm the outcome of synthesized MR fluids, a MR brake test rig has been developed; experiments have been performed; and the results of braking torque and temperature distribution are presented. The surface temperature of MR brake housing have been measured using eight thermocouples. The MR brake has been operated in “shear” and “compression assisted shear” modes as detailed in the literatures [1, 12]. The results of temperature distribution and torque using various MR fluids have been compared and presented.

II. Synthesis and Characterization

In this research work, four MR fluid samples have been synthesized using microns sized (3 to 394 microns) carbonyl iron (purity 99%) particles purchased from SIGMA ALDRICH. The particle size distributions were measured using HORIBA Laser Scattering Particle Size Distribution Analyzer LA-950. The probability volume density graph of iron particles are shown in Figure 1. For MR brake or clutches applications where two rotating bodies are relatively moving (mechanical stirring action), sedimentation is not a problem. One percent impurities, in iron sample, contain As: ≤5mg/kg, Cu: ≤100 mg/kg, Mn: ≤1000 mg/kg, Ni: ≤500 mg/kg, Pb: ≤20 mg/kg and Zn: ≤50 mg/kg.

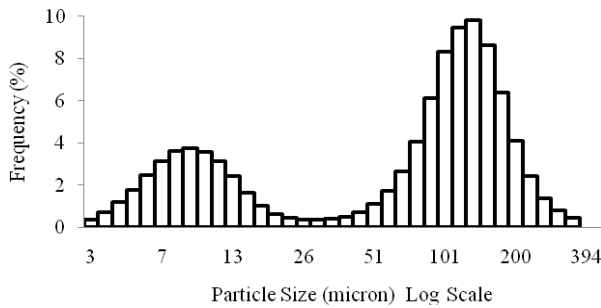


Fig 1. Probability volume density graph of particle sizes

First MR fluid sample MRF85 contains 14.5% by wt silicone oil, 0.5% by wt oleic acid, and 85% by wt carbonyl iron powder as indicated in Table 1. Similarly three other MR fluid samples contain 0.5% by wt oleic acid, 85% by wt carbonyl iron powder, specification of which is listed in Table 1.

Table 1. MR fluid compositions

MR fluids samples	Silicone Oil (%) by wt.)	Iron particle (% by wt)	Oleic acid (% by wt)	Cu nano powder (% by wt)
MRF85	14.50	85	0.50	0
MRF85_0.25Ag	14.25	85	0.50	0.25
MRF85_0.50Ag	14	85	0.50	0.50
MRF85_0.75Ag	13.75	85	0.50	0.75

Copper nano-powder suspensions, purchased from Reinste Nano Ventures, contains copper particle size of 40 ± 5 nm in ethanol (30 % by weight) and metal impurities lesser than 0.1% including Fe ($<0.02\%$). The shear stress of MRF85, MRF85_0.25Cu, MRF85_0.50Cu and MRF85_0.75Cu at various magnetic fields measured using magnetorheometer ANTON PAAR MCR-102, are plotted in Figure 2. The shear stress of each sample was measured thrice. From figure 2, it can be inferred that the shear stress of all four MR fluids samples lie within the error bar. There is no significant variation in the stress values. To explore the spread of copper on iron particles, SEM and EDX of MR particles was performed.

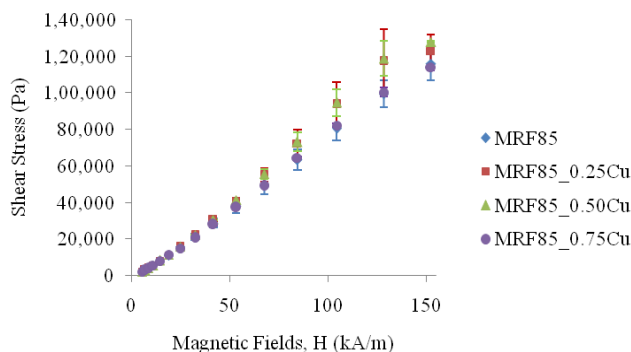
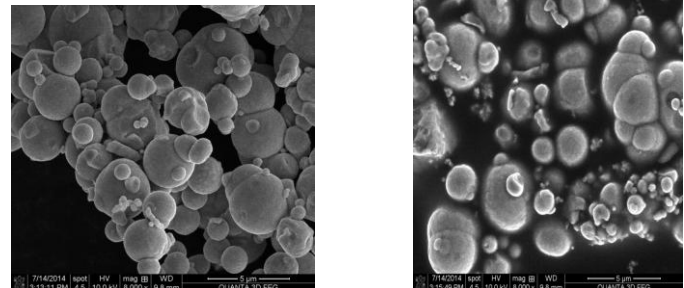


Fig 2. Shear stress of MR fluids at various magnetic fields

The scanning electron micro scope photographs of iron particles (Sigma Aldrich) are shown in Figure 3(a). These iron particles of different sizes are nearly spherical in shape. The iron particles extracted from MRF85_0.75Cu, and the scanning

electron microscopic photograph of this iron particles have been captured and shown in Figure 3(b). It shows that Cu nano powder make a layer over the iron particles. Figure 4 shows EDX analysis of extracted iron particles from MRF85_0.75Cu. It confirms the presence of Cu nano powder with the iron particles.



(a) Iron particles (Sigma Aldrich) (b) Iron particles coated with Cu nano-powder

Fig 3. Scanning electron microscopic photograph of iron particles coated and uncoated

To observe the effect of temperature rise on the shear stress of MR fluids, all four samples were subjected to temperature 30, 35, 40, 45, 50 and 55 degree centigrade. The results of shear measured at those samples are plotted in Figure 5.

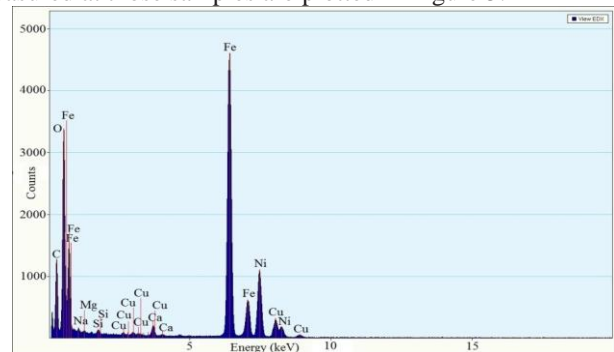


Fig 4. EDX analysis of extracted iron particles from MRF85_0.75Cu

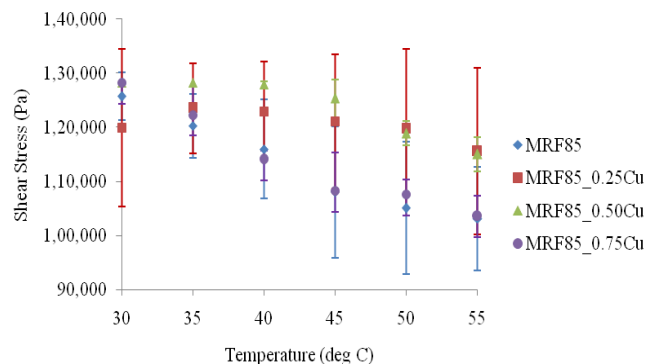


Fig 5. Thinning of MR fluids at different temperatures

Figure 5 shows the thinning behaviour of the four MR fluids with increase in temperature. It can be said that shear stress of all MR fluids decreases with increase in temperature. To validate the shear stress results of MR fluids, performance of MR brake has been carried in experimental test rig.

III. Design and development of MR brake operating under shear and compression assisted shear modes

A schematic of proposed MR brake is shown in Figure 6. Rod seal has been used to stop the leakage of MR fluid. The stator is mounted on the bearing. A side electromagnet has been used to slide the housing plate towards the disk to compress the MR fluid. Both the stator and housing plates are made of low carbon steel. The shaft is made of stainless steel.

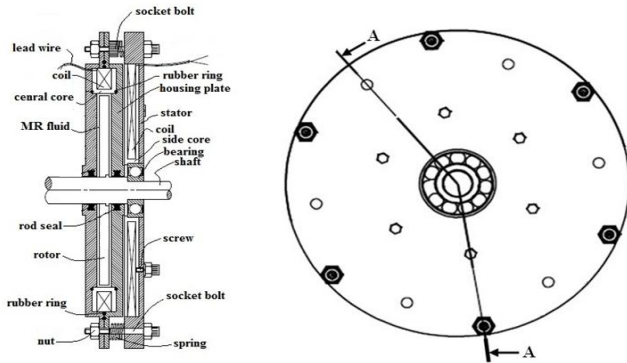


Fig 6. Schematic drawing of MR brake

A schematic of MR brake, developed in the present study has been shown in Figure 7. Initially, in the absence of current supply in the coil of central core, MR particles remain uniformly distributed in the fluid as shown in Figure 7. Figure 8 depicts the alignment of MR particles in the direction of magnetic field when the current is supplied in the central electromagnet. These MR particles make chains/clusters to resist the motion of disk and such braking action from MR brake is named as “shear mode” of MR brake.

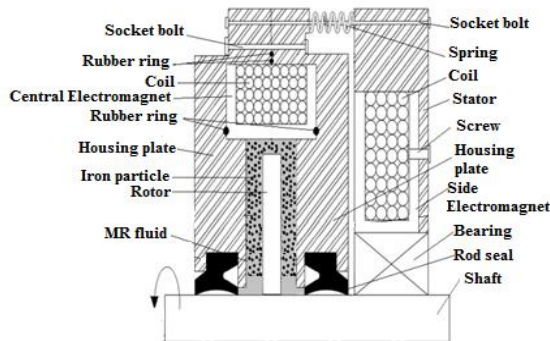


Fig 7. Random distribution of iron particles

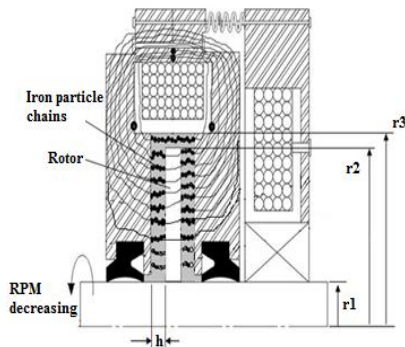


Fig 8. Chain of iron particle in MR brake

When current is gradually applied in the side electromagnet, the stator acts as a magnet and the housing plate assembly acts as an armature which slides in the direction D_a by compressing the springs as shown in Figure 9. When current is applied in the central electromagnet, compressed iron particles make stronger chains in the compression zone and weak chains in the expansion zone. Such braking action is named as “compression assisted shear mode” of MR brake.

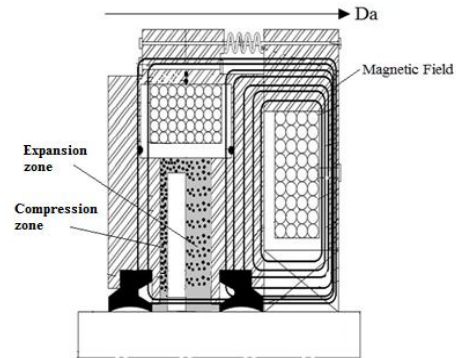


Fig 9. Iron particle after compression

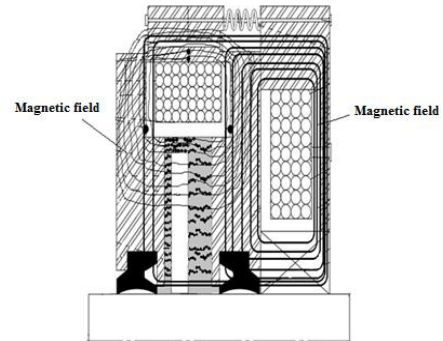


Fig 10. Iron particle chain after compression

IV. Experimental study on MR brake

The block diagram of the MR brake test rig is shown in Figure 11. It comprises of 3-phase 5-HP D.C. motor with speed controller, jaw coupling, a flywheel (20kg), and MR brake through bearing brackets. A D.C. (30 V and 5 A) power supply has been used to regulate the current in the electromagnet of MR brake. A tachometer has been used to measure the rotational speed. A number of experiments at various operating conditions (magnetic field 0 to 300 kA/m and speed 200 and 600 rpm) have been performed.

After completing each experiment, a table fan was used to reduce the time to cool brake back to the room temperature. Figure 12 displays the MR brake test rig. Figure 13 illustrates the position of the thermocouples on the surface of the MR brake housing. Eight thermocouples have been used to measure the localized temperature on the surface of the housing of MR brake. The rotor has inner radius (r_1) 10 mm and outer radius (r_2) 44 mm. Three thermocouples have been installed at minimum P.C.D (24mm) and five thermocouples have been installed at the maximum P.C.D (80mm) on the housing surface at equal distance so that the temperature can be measured at the

housing surface area where MR fluids make a chain between the housing and rotor.

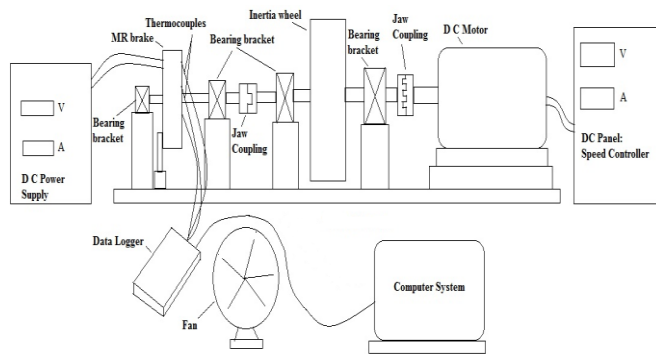


Fig 11. Schematic diagram of the MR brake test rig

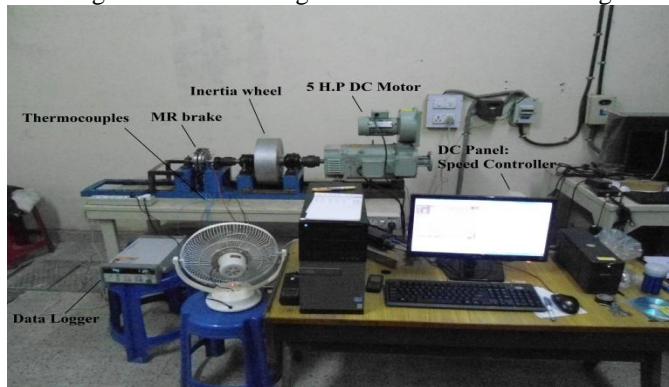


Fig 12. Photograph of MR brake test rig

The present setup can be used to find braking torque under “shear mode” as well as “compression assisted shear mode”. To evaluate the brake torque and temperature rise at any particular speed (i.e. 200 rpm, 600 rpm) in shear mode, following procedure have been charted:

- Maintain the motor speed at the specified rpm using speed controller. Record the readings of voltmeter and ammeter to estimate the power supplied. Use the tachometer to measure the speed of the brake shaft.
- Supply current to the central electromagnet of MR brake. In the presence of magnetic field, MR brake reduces the speed of the motor.
- Increase the voltage of the speed controller to maintain the specified speed (RPM) of the MR brake shaft. Record the new readings the voltmeter and ammeter to estimate the final supplied power. Estimate braking torque using $BT = (PW_f - PW_i) / \omega$. Here, PW_i and PW_f are initial and final power loss; ω is the specified angular speed.
- After stabilization of temperature, record the readings of thermocouples in the desktop computer using data logger.
- Switch off the power supply to the electromagnet and reduce the RPM of the DC motor to zero.
- Switch on table fan to cool the MR brake to get back to initial temperature. Repeat the same procedure for another

experiment (different current to electromagnet and different motor speed).

- Similar procedures have been used to find braking torque “compression assisted shear mode” except one additional step of supplying the desired current in the side electromagnet to compress the MR fluid and then supplying the desired current in central electromagnet.

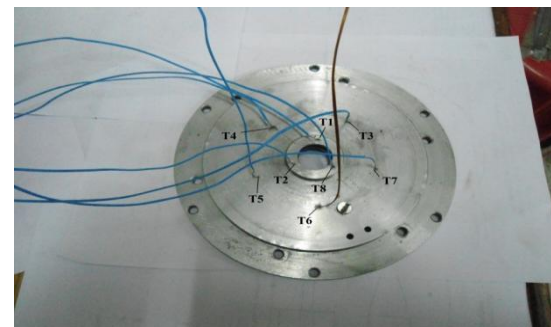


Fig 13. Position of thermocouples (T1, T2, T3, T4, T5, T6, T7, T8) on the surface of the brake housing

V. Results and Discussions

Figures 14 shows the braking torque and surface temperature of the MR brake housing using two MR fluids (MRF85 and MRF85_0.25Cu) in shear mode at 200 RPM. For both the fluids increase in braking torque as well as temperature with increase in current supplied to the central electromagnet can be noticed. It is important to notice that the braking torque for both MR fluids is same. Temperature of the MR brake containing MRF85 is higher than that of MRF85_0.25Cu. This proves that the heat transfer rate of the MRF85_0.25Cu is higher than that of MRF85.

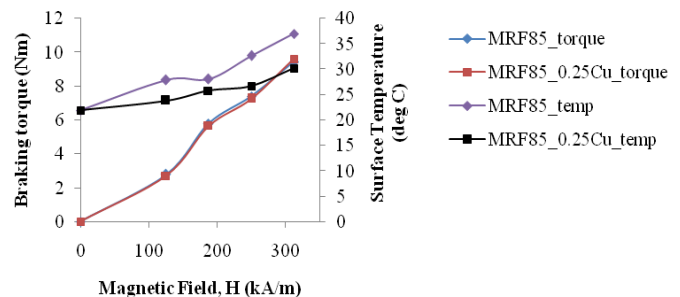


Fig 14. Braking torque and surface temperature in shear mode at 200 RPM

Figure 15 shows the braking torque and surface temperature of the MR brake in “compression assisted shear mode” at 200 RPM. As per the Figure 15, there is insignificant difference in torque exerted using MRF85 and MRF85_0.25Cu based MR brakes. It is worth noting that braking torques under “compression assisted shear mode” (Figure 15) are higher compared to that obtained under shear mode (Figure 14). Another important observation is reduction in surface temperature in “compression assisted shear mode” compared to “shear mode” of MR brake. This indicates that due to compression of MR fluids, heat dissipation rate increases. The heat transfer mechanism of compressed iron particles of MR fluids is shown in Figure 16.

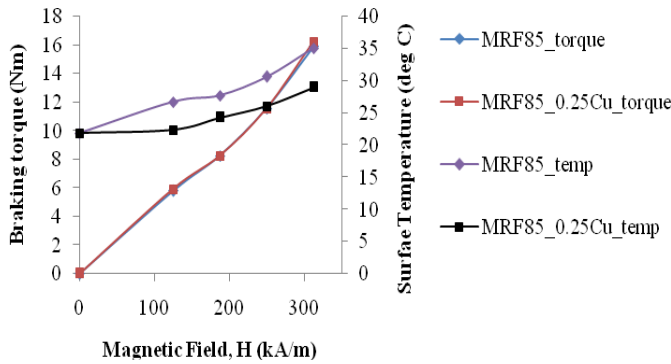


Fig 15.Braking torque and surface temperature in compression assisted shear mode at 200 RPM

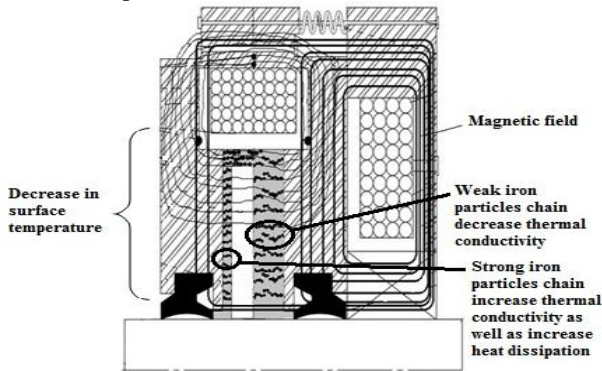


Fig 16.Heat Transfer mechanism of MR brake

At 200 RPM, the braking torque of MR brake in shear mode for MRF85 and MRF85_0.25Cu are 9.45 Nm and 9.62 Nm respectively. The surface temperature for MRF85 and MRF85_0.25Cu are 37.04°C and 30.18°C in shear mode. In compression assisted shear mode, the braking torque of MR brake for MRF85 and MRF85_0.25Cu are 15.89 Nm and 16.26 Nm respectively, whereas the surface temperature for MRF85 and MRF85_0.25Cu are 35.07 °C and 28.94°C respectively. There is 1.79% increase in braking torque with 22.73% decrease in surface temperature using copper nano powder in MR fluids in shear mode at 200 RPM and 2.23 % increase in braking torque with 17.49 % decrease in surface temperature in “compression assisted shear mode”.

In order to capture the performance of MR brake at higher speed, experiments were performed at 600 rpm speed. The braking torque and surface temperature in “shear mode” and “compression assisted shear mode”, have been measured and plotted in Figure 17 and Figure 18. At 600 RPM, the braking torque in shear mode for MRF85 and MRF85_0.25Cu are 7.67 Nm and 7.74 Nm respectively. The surface temperature for MRF85 and MRF85_0.25Cu are 54.05°C and 45.32°C in shear mode. In compression assisted shear mode, the braking torque of MR brake for MRF85 and MRF85_0.25Cu are 9.31 Nm and 9.67 Nm respectively, whereas the surface temperature for MRF85 and MRF85_0.25Cu are 41.89°C and 38.82°C respectively. It shows that the braking torque decreases with increase in the speed.

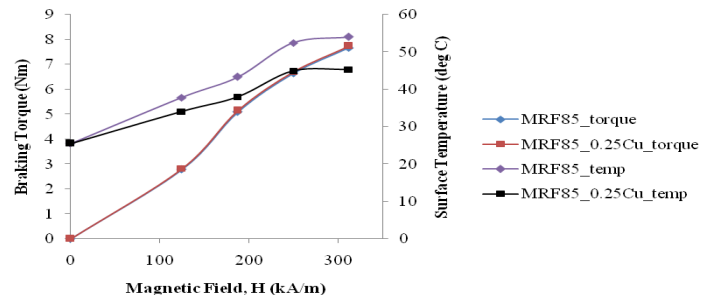


Fig 17.Braking torque and surface temperature in shear mode at 600 RPM

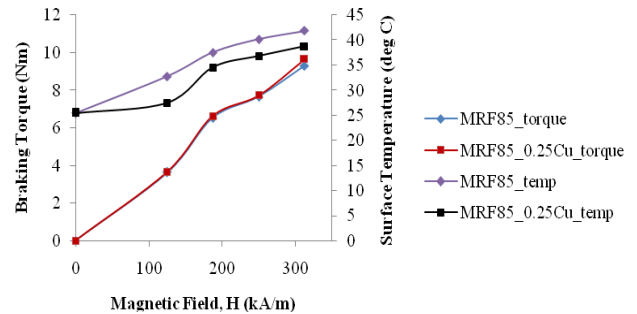


Fig 18.Braking torque and surface temperature in compression assisted shear mode at 600 RPM

To observe the effect of 0.50% Cu and 0.75% Cu, the experiments on MR brake using MRF85_0.50Cu and MRF85_0.75Cu have been performed. Figure 19 and Figure 20 show the braking torque and maximum surface temperature of housing using four MR fluid samples at 600 RPM in “shear” and “compression assisted shear” modes, respectively. The braking torque and maximum localized surface temperature for MR brake containing MRF85, MRF85_0.25Cu, MRF85_0.50Cu and MRF85_0.75Cu are 7.67 Nm, 7.74 Nm, 7.74 Nm and 7.70 Nm respectively in shear mode and 54.05°C, 45.32°C, 41.45°C and 38°C respectively. The braking torque and maximum localized surface temperature using MRF85, MRF85_0.25Cu, MRF85_0.50Cu and MRF85_0.75Cu are 9.31 Nm, 9.67 Nm, 9.67 Nm and 9.54 Nm respectively in compression assisted shear mode and 41.89°C, 38.82°C, 37.77°C and 36.12°C respectively.

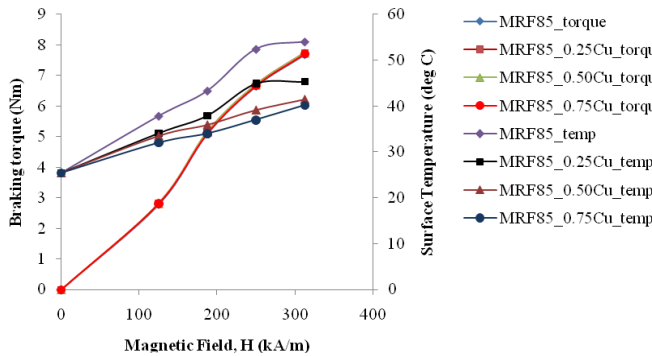


Fig 19.Braking torque and surface temperature using four different MR fluids in shear mode at 600 RPM

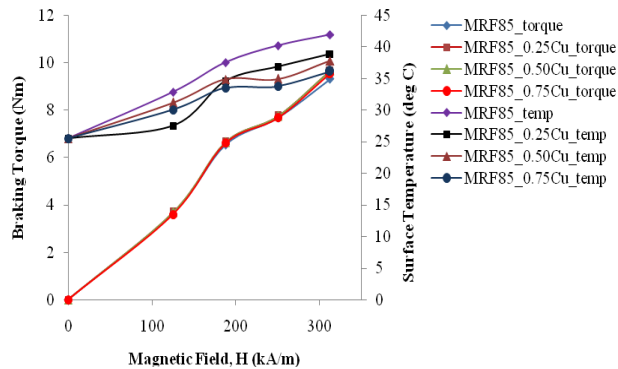
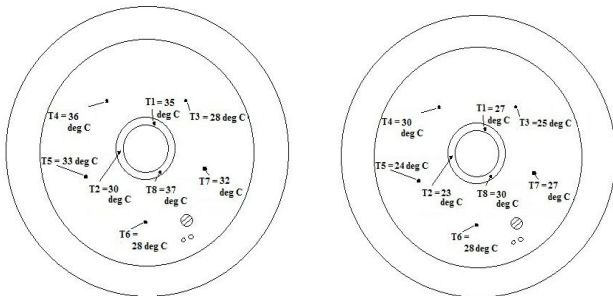
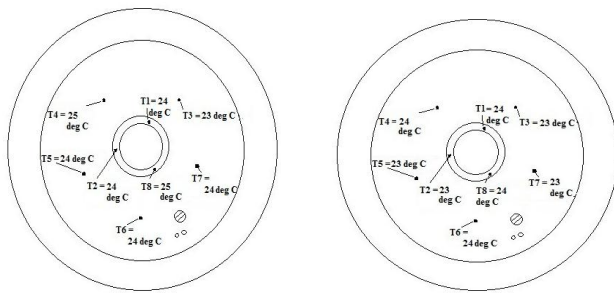


Fig 20.Braking torque and surface temperature using four different MR fluid samples in compression assisted shear mode at 600 RPM



(a) MRF85 (b) MRF85_0.25Cu

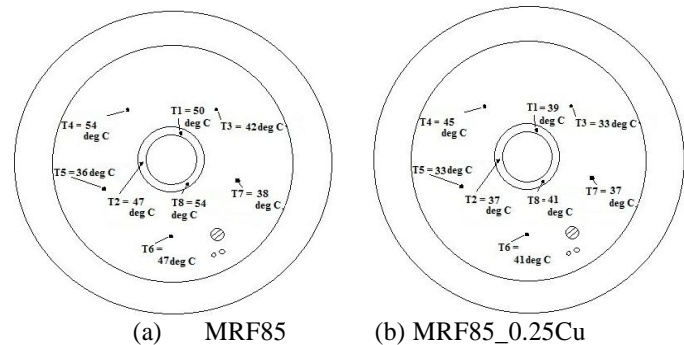
Fig 21.Thermocouple readings using MRF85 and MRF85_0.25Cu at 200 RPM



(a) MRF85_0.50Cu (b) MRF85_0.75Cu

Fig 22.Thermocouple readings using MRF85_0.50Cu and MRF85_0.75Cu at 200 RPM

Figure 21 and Figure 22 show the thermocouple readings (at maximum magnetic field in shear mode) using MRF85 and MRF85_0.25Cu samples at 200 RPM; using MRF85_0.50Cu and MRF85_0.75Cu samples at 200 RPM respectively. Figure 23 and Figure 24 show the thermocouple readings (at maximum magnetic field in shear mode) using MRF85 and MRF85_0.25Cu samples at 600 RPM; using MRF85_0.50Cu and MRF85_0.75Cu samples at 600 RPM respectively. On the basis of Figure 21, Figure 22, Figure 23 and Figure 24 it can be said that increase in percentage (0 to 0.75) of copper nano-powder reduces the temperature of brake surface. The maximum temperature of the surface MR brake in shear mode without Cu nano-powder is 54°C while the maximum temperature of MR brake with 0.75% Cu nano-powder is 40.15°C. It can be said that the nano-copper powder increases the heat transfer rate of MR fluid. This method of cooling MR fluid is economic and better (in terms of required geometrical space) than other cooling methods [5, 8-10]. The Cu based MR fluids shall be used if there is a need to impart the cooling capabilities in MR fluid devices. The variation of the temperature of thermocouples indicates that there is some misalignment between the disk and MR brake housing.



(a) MRF85 (b) MRF85_0.25Cu

Fig 23.Thermocouple readings using MRF85 and MRF85_0.25Cu at 600 RPM

VI. Conclusions

In the present manuscript effects of copper nano powder on the shear stress and heat transfer rate of MR fluid have been explored. Four MR fluid samples were synthesized. Shear stresses of all synthesized MR fluids at various temperatures were measured using MCR-102 magnetorheometer. Each experiment was repeated thrice and no significant change in shear stress due to mixing of MR fluid was observed. In other words, shear stress of MR fluids does not decrease with increase in weight percentage of copper nano-powders. To observe the increase in heat transfer rate due to mixing of copper nano powder, MR brake test rig was been developed. Experiments performed on MR brake rig indicate that on increasing copper nano-powder percentage, surface temperature of MR brake decreases. Based on these results it can be concluded that the use of Cu nano-powder is effective cooling method. It does not require any extra space to cool the MR brake. The Cu based MR fluids shall be used if there is a

need to impart the cooling capabilities in MR fluid devices.

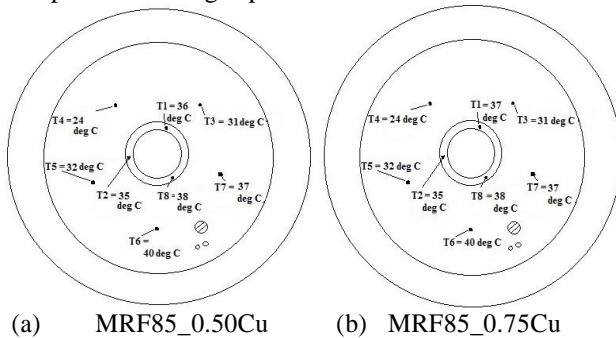


Fig 24. Thermocouple readings using MRF85_0.50Cu and MRF85_0.75Cu at 600 RPM

REFERENCES

- i. Sarkar, C. and Hirani, H. Theoretical and experimental studies on a magnetorheological brake operating under compression plus shear mode, *Smart Mater. Structure*, 2013, 22, 115032 (12pp).
- ii. Karakoc, K.; Park, E. J. and Suleman, A. Design considerations for an automotive magnetorheological brake, *Mechatronics*, 2008, 18, 434–47.
- iii. Li, W. H. and Du, H. Design and experimental evaluation of a magnetorheological brake, *Int. J. Adv. Manuf. Technol.*, 2003, 21, 508–15.
- iv. Nam, T. H. and Ahn, K. K. A new structure of a magnetorheological brake with the waveform boundary of a rotary disk, *Smart Mater. Struct.*, 2009, 18, 115029 (14pp)
- v. Wang, D. M.; Hou, Y. F.; and Tian, Z. Z. A novel high-torque magnetorheological brake with a water cooling method for heat dissipation, *Smart Mater. Struct.*, 2013, 22, 025019 (11pp).
- vi. Wiess, K. D. and Duclos, T. G. Controllable fluids: the temperature dependence of post-yield properties., *Int. J. Mod. Phys. B.*, 1994, 8, 3015-32.
- vii. Liao, C. R. Study on Magnetorheological Fluid Damper for Automobile Suspension System, 2001 (Chongqing: Chong Qing University) (in Chinese)
- viii. Dogruoz, M. B.; Gordaninejad, F.; Wang, E. L. and Stipanovich, A. J. Heat transfer from fail-safe magnetorheological fluid dampers, *Proc. SPIE Conf. Smart Mater. Struct.*, 2001, 4331, 343–353.
- ix. Tian, Z. Z. and Hou, Y. F. A double-disk magnetorheological clutch, CN Patent Application 201110041597, 2011.
- x. Zheng, J.; Zhang, G. H. and Cao, X. J. Design and experiment for magnetorheological transmission device with heat pipes, *Chin. J. Mech. Eng.*, 2009, 45, 305–311.
- xi. Mistik, S. I.; Shah, T.; Hadimani, R. L. and Siores, E. Compression and thermal conductivity characteristics of magnetorheological fluid-spacer fabric smart structures, *J. Int. Mater. Syst. and Struct.*, 2012, 23, 1277-1283.
- xii. Sarkar, C. and Hirani, H. Design of a squeeze film magnetorheological brake considering compression enhanced shear yield stress of magnetorheological fluid, *Journal of Physics: Conference Series*, 2013, 412, 012045 (12pp).